Influence of polydimethylsiloxane addition on the sintering behavior of the fused silica bodies

Shadi Behsam[1], Mahboubeh Rezaei[1], Mahshid Saghatchi[2], Adrine Malek Khachatourian[1,*], Sorosh Abdollahi[2], Amirhosein Paryab[1]

[1]*Department of Materials Science and Engineering, Sharif University of Technology, Tehran, Iran*

[2]*School of Metallurgy and Materials Engineering, Iran University of Science and Technology, Tehran, Iran*

Received 6 November 2024; received in revised form 14 March 2025; accepted 19 March 2025

Abstract

Fused silica materials are of high importance because of their excellent thermomechanical properties. So far, fused silica bodies have been produced mostly through solid-state sintering of slip-cast bodies. Herein, a novel processing route based on the polymer-derived ceramic (PDC) method for the fabrication of porous fused silica bodies was presented for the first time. In this method, the key to fabricating these bodies is to use polydimethylsiloxane (PDMS) as a source of silica and a binder to provide formability and green strength besides of fused silica aggregates. It was revealed that this method provides porous bodies with up to 24 vol.% porosity and relative low strength. It was shown that the addition of PDMS helps with the sintering of the bodies at temperatures ≥1200 °C by increasing the density and strength due to their melting and infiltration inside the pores. It was also noted that the addition of PDMS increases the tendency of the system to crystallization.

Keywords: *fused silica, polymer-derived ceramics, polydimethylsiloxane, liquid phase sintering*

I. Introduction

Advanced ceramics have a phenomenal role in developing advanced materials with great functionalities [1]. Among various advanced materials, fused silica has attracted extensive attention in applications such as cores in the casting of super alloys [2] mostly due to its high thermal shock resistance, high strength at elevated temperatures, high chemical resistance, thermal stability and refractoriness [3]. Moreover, fused silica has been found useful in applications like space shuttle windows, deep UV lens elements and optical fibres due to its high resistance to optical damage, high refractive index homogeneity and large transparency range [4]. Fused silica materials have also been utilized for semiconductor and photovoltaics (PV) applications such as high-purity fused silica crucibles for Czochralski silicon (Cz-Si) growth, parts for etching or cleaning and tubes for annealing [5]. Fused silica substrates showed great potential for developing laser-based multifunctional thermal-control microfluidics [6].

*Corresponding author: tel: +48 504 745 364
e-mail: *khachatourian@sharif.edu*

Fused silica bodies are mainly fabricated through slip-casting methods, in which wet milling is first done to yield an ideal particle size distribution. Then, its viscosity is controlled to stabilize the slip. After casting, the drying and sintering procedures are conducted to achieve the final product [7]. Also, several other forming methods exist, which are less common, like cold press [8] and gel-casting [9]. Some other techniques involving simultaneous shaping and sintering have been reported, such as spark plasma sintering [10], hot-press [11], hot isostatic press [12] and flash sintering [13]. Two phenomena occur during the sintering: the first, upon sintering the mechanical strength of the material increases due to the densification of the system, and the second, the crystallization of the most stable form of crystalline silica at high temperature, β-cristobalite phase [14,15]. It is well known that densification is a positive issue while crystallization is not, mainly because it changes the sintering mechanism from viscous flow to diffusion, which is less efficient. Moreover, β-cristobalite undergoes a phase transformation that induces strains at the interface of glass-cristobalite and creates microcracks, giving rise to strength deterioration [16].

Kazemi *et al*. [17] investigated the cristobalite crystallization of fused silica-based ceramic cores formed through injection molding. They reported that in-situ cristobalite crystallization occurs at 1380 °C on the surface of fused silica grains, decreasing the flexural strength and leachability. Moreover, the addition of alumina enhances the cristobalite crystallization. Manivannan *et al*. [18] used the gel-casting method with colloidal silica as the binder and a solid loading of 73% to fabricate fused silica samples sintered at 1200 °C for 2 h. The sintered samples retained their amorphous nature and achieved 95 % of the theoretical density and flexural strength of 60 MPa. Dehghani *et al.* [15] sintered fused silica samples formed with slip casting at 1100 to 1400 °C. They reported that the density, cristobalite phase content and dielectric constant increased with increasing temperature, while the highest strength (48.7 MPa) was achieved at 1300 °C. In another study, Dehghani *et al*. [10] fabricated and sintered fused silica powders with different particle sizes using the SPS method at 900 to 1300 °C. They reported that density and cristobalite phase content increased upon increasing temperature and reducing initial particle size. The highest bending strength (40 MPa) was reported to be of the sample with coarser powder plasma-sintered at 1100 °C.

The polymer-derived ceramic (PDC) method has emerged recently as a promising method for the fabrication and sintering of ceramic bodies [19]. In this method, a preceramic polymer source is prepared, which is usually blended with ceramic fillers [20]. The polymer is then cured, and the whole blend is shaped to form the desired geometry. Then, the system undergoes heat treatment and the polymer decomposes in a process referred to as ceramization [21]. It is obvious that the main advantage of this method is the ability to form precursors in the plastic state through methods like injection moulding. Also, the atomic scale homogeneity of the blend requires less heat treatment temperatures than conventional solid-state methods [22]. It is also anticipated that this method yields porous bodies, primarily due to the sublimation of gasses produced from polymer decomposition [23,24].

In the present study, the novel PDC method for the fabrication of porous fused silica bodies has been introduced. As presented in previous publications, a precursor polymer material like polydimethylsiloxane (PDMS) is dissociated in the air when heated at 450 °C and forms amorphous silica submicron particles [25]. Herein, the PDMS polymer was blended with fused silica particles at specific ratios and underwent heat treatment in the air at different temperatures. The merit of this method is the deformability and capability of the blend, which helps in methods like injection moulding, casting, etc. The goal of this work was to assess how the fine submicron silica derived from PDMS could influence the sintering of coarse fused silica particles and how the crystallization of the system underwent changes. The effect of heat treatment temperature and the fused silica to PDMS ratio on the sintering and crystallization was studied. Since the inorganic content of the polymer was around 50%, it is evident that a massive proportion of the polymer turned into empty space. Thus, higher fractions of PDMS than 20% were not possible due to the deformation of the samples. Then, structural, microstructure, physical, and mechanical properties of fabricated samples were investigated.

Table 1. Chemical composition and final heat treatment temperature of the fabricated samples

Sample	Chemical composition		Final heat treatment temperature [°C]
	PDMS [wt.%]	Fused silica [wt.%]	
FS1100	10	90	1100
FS1150	10	90	1150
FS1200	10	90	1200
FS1250	10	90	1250
FS1300	10	90	1300
FS80201200	20	80	1200

II. Experimental

2.1. Fabrication of porous fused silica bodies

All precursors used in this work are of commercial grade and used without purification. Commercial fused silica (Pooyandegan Sanat Aria Co., with average particle size of 44 μm and 99.8% purity) was employed as an inorganic part. Commercial RTV2 silicone resin (PDMS with 99.999% purity) accompanying a liquid hardener, xylene as a solvent and Span 80 as a surfactant were used as the organic part. The chemical composition of each sample and its processing temperature are presented in Table 1. First, silicone resin is poured inside a small beaker. Then, 20 wt.% xylene and 2 wt.% Span 80 (dispersing agent) relative to the whole batch were added to the system to dilute the resin and disentangle the polymer chains. After that the fused silica was added slowly and if the system could not mix well, more xylene was added. Then, the beaker was put on a heater to evaporate the solvent, and stirring continued throughout the process. Finally, the hardener was added to the system (in

amount equivalent to 5 wt.% of the used polymer) with continuous stirring. After 5 min, the mixtures were poured inside ruler-shaped moulds, kept outside for 2 h and transferred to a furnace for sintering. The materials were heated at the rate of 5 °C/min until 400 °C and at the rate of 0.5 °C/min (the lower rate is used because of the polymer dissociation and gas sublimation) until 550 °C. Soaking times were 30 min at 400 and 550 °C to ensure the pyrolysis process was terminated. Finally, the obtained as-received silica samples were heated to the final temperature at 5 °C/min rate and soaking time of 60 min. Figure 1 shows the scheme of sample fabrication.

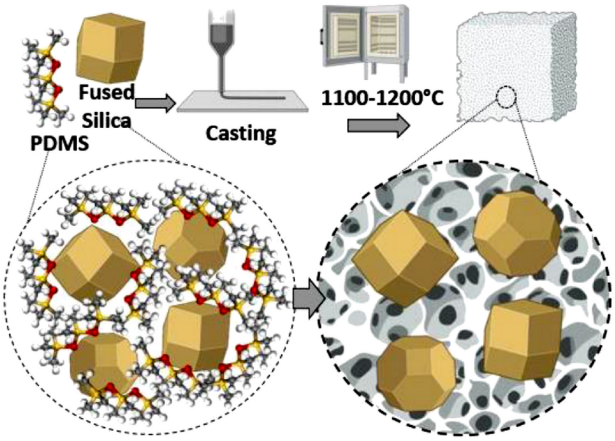

Figure 1. Scheme of sample fabrication

2.2. Structural and microstructural evaluations

Differential scanning calorimetry (DSC) was conducted with regard to ASTM E1131 by Mettler Toledo up to 600 °C in air atmosphere with 10 °C/min. The density and open porosity of the samples were computed according to the ASTM C373 protocol, whereas the closed porosity was calculated by the difference between the total porosity and the open porosity. The total porosity was calculated by considering the ratio between the bulk density and theoretical density of the glass-ceramics, which is itself calculated by taking in account the real densities of fused silica and cristobalite. In order to examine the phase evolution during heat treatment and identify the crystalline phases, the phase analysis was carried out using X-ray diffraction (XRD; Panalytical-2009, Cambridge, U.K.) with Cu Kα radiation (λ = 0.15418 nm). Also, the Rietveld refinement technique was employed for the quantitative phase analysis. A field emission electron microscope (FESEM; TeScan Mira III, Brno, Czech Republic) was used to conduct the microstructural evaluations. For thermal shock resistance evaluation, the samples were heated at 1000 °C for 10 min and then cooled abruptly in water at room temperature. Flexural strength (Modulus of rupture, MOR test) was measured according to the ASTM C583 using an eXpert 8600 device. The cycle was repeated 3 times, and then MOR and reduction in MOR were measured and reported. Each test was repeated 3 times.

III. Results and discussion

Behaviour of the pure PDMS upon heat treatment up to 600 °C was investigated by DSC and shown in Fig. 2a. In the temperature range from 25 to 300 °C solvent, small organic moieties and hardener burned and sublimated from the sample. Strong exothermal effect was observed in the temperature range from 420 to 550 °C and indicates the reaction of silicone polymeric chains with the oxygen and formation of silica. XRD pattern of the as-received fused silica material, presented in Fig. 2b, confirms the highly amorphous structure with a broad peak at 2θ ~20°. It is in accordance to the literature data [14], which confirmed that the crystallization in this system starts at temperature above 1100 °C.

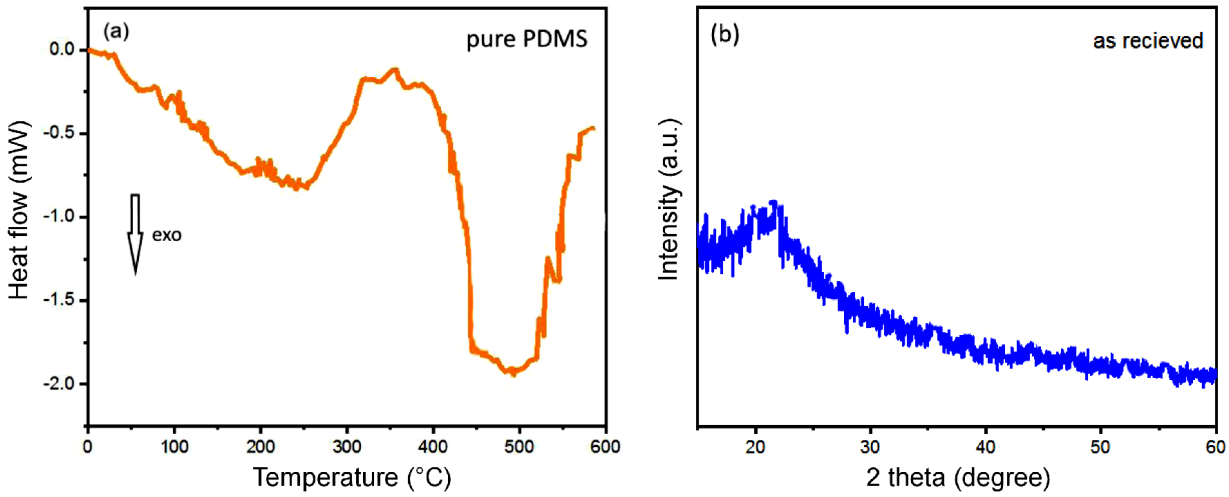

Figure2. DSC analysis of pure PDMS (a) and XRD pattern of as-received fused silica (b)

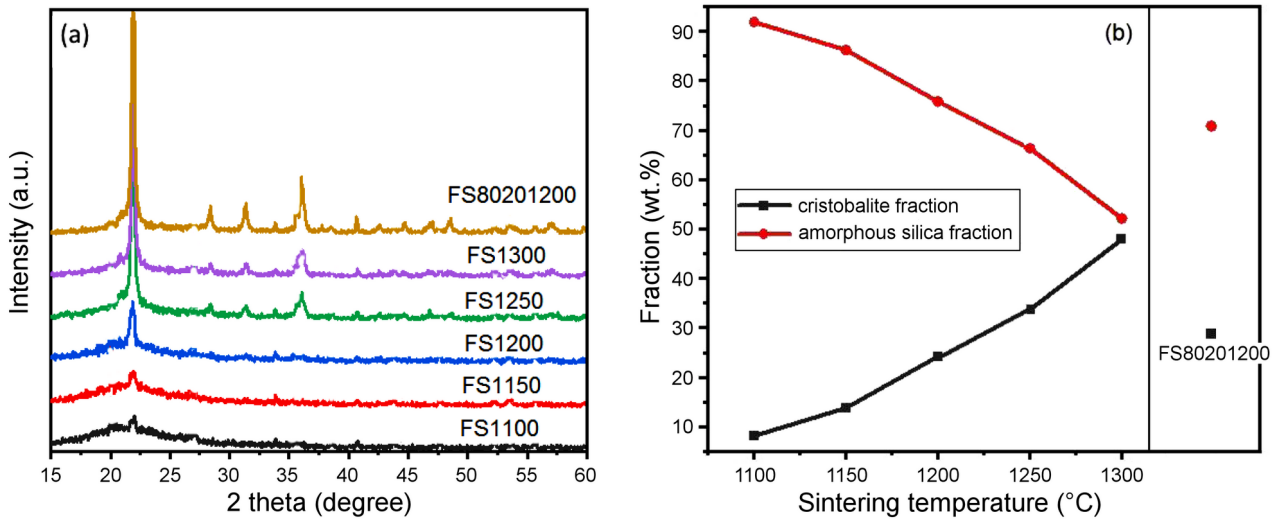

Figure 3. XRD patterns of sintered samples (a) and the quantitative phase analysis by Rietveld refinement (b)

Figure 3 demonstrates XRD results of the fabricated samples accompanied by the Rietveld quantitative analysis. According to Fig. 3a, upon increasing the temperature, a ratio of the amorphous phase of the fused silica turns into a crystalline cristobalite phase (JCPDS 04-008-7642), which is widely accepted in the literature [10,16,18,26]. However, unlike other works, in this work, 5–10 wt.% of the whole silica (after pyrolysis) is supplied by PDMS.

It was known from the previous work [25] that silica derived from PDMS is not crystallized below 1050 °C and in our case XRD results revealed that the PDMS-derived silica crystallizes at 1100 °C and above. Since the PDMS-derived silica particles have submicron size and their surface area is much higher than of the fused silica particles (filler), it can be concluded that their tendency for crystallization must be higher than fused silica. This is mainly due to the surface nucleation of crystals, which is preferred in this system [27,28]. Thus, the broad peaks of cristobalite at lower temperatures prove their small crystal size and low crystallinity of the PDMS-derived silica. According to above discussion, more cristobalite phase can be expected in the FS80201200 than in the FS1200 sample, what was confirmed by XRD results (Fig. 2a). Thus, one theory is plausible here, which is as follows: upon increasing the temperature to 1200 °C, submicron PDMS-derived silica was able to melt and diffuse across the surface of fused silica particles and form a layer on them. Apart from the role of this phenomenon on mechanical strength, which will be addressed in the following parts of the article, it could positively or negatively influence the crystallization of the fused silica. Since higher amounts of cristobalite were detected in this work compared with the literature [26], it is possible that the PDMS-derived silica layer on the surface of fused silica encouraged the crystallization.

Figure 4 shows the results of the physical properties assessments of the samples. Figure 4a demonstrates the results of bulk density, open and closed porosity. The bulk density of the samples was in the range of 1.48–1.66 g/cm^3, which is consistent with the results of the same materials made through gel-casting [9,16]. However, it is much lower than those slip-casted [29] or pressed specimens [26], which are in the range of 1.8–2.0 g/cm^3. The density of the samples increased with temperature (Fig. 4a) due to the higher diffusion rate and viscous flow. Nonetheless, the crystallization lowers the sintering efficiency by changing the sintering mechanism and makes the microstructure more porous, since the crystals grow in an anisotropic way in various directions. However, in this case, the density increase is due to the sintering effect, which dominated the decrease in density due to crystallization.

It was noticed that although polymer content in the FS80201200 sample is twice as much as the FS1200 sample, its density is not much lower. This can be explained by the same theory explained above. The PDMS-derived silica was melted at temperature ≥1200 °C and since its amount is higher in the FS80201200 sample, it could fill the pores to some extent by viscous flow mechanism. Until 1250 °C, the open porosities decrease and turn into closed porositie, and at 1300 °C this trend reverses (i.e. closed porosities become open) due to further process of crystallization.

Figure 4b indicates the evolution of flexural strength before and after thermal shock. Overall, thermal shocks deteriorate the MOR and the amount of strength reduction is proportional to the amount of cristobalite. The strength amounts before thermal shocks correspond with the density of the samples and the amount of their cristobalite contents, which increase and decrease the strength, respectively. Before 1250 °C, the densification has dominant

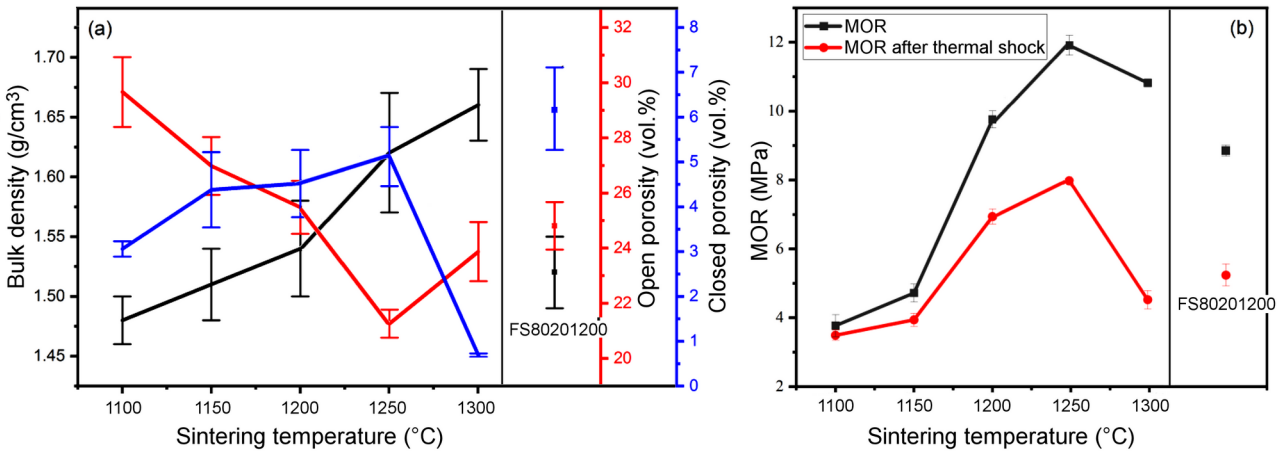

Figure 4. Density and porosity (a) and MOR results of fabricated samples before and after the thermal shock (b)

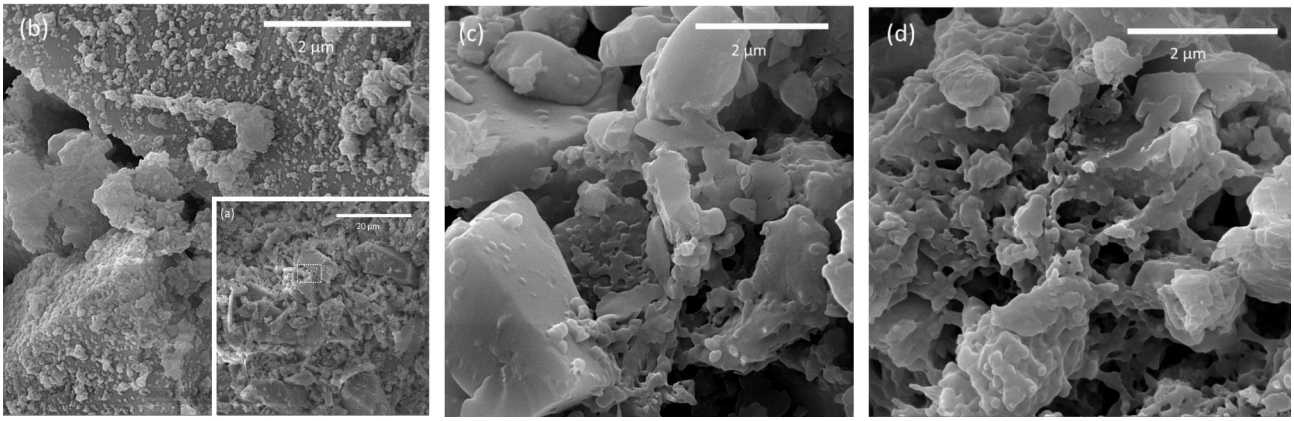

Figure 5. FESEM micrographs of: a) FS1100 (with and enlarged area), b) FS1200 and c) FS80201200

contribution in determining the MOR, while after that this role is taken over by crystallization. The strength of the FS80201200 sample is lower than that of the FS1200 ceramics, which is expected considering its lower density and higher cristobalite content. Overall, MOR values of the fabricated samples by this method are lower than that of the pressed and slip-casted samples due to the lower compaction of particles (i.e. lower densities). The low-toxicity monomer N-dimethyl acrylamide (DMAA) was used in the gel casting of fused silica glass by Wang *et al*. [30] and maximal density and flexural strength of fused silica glass sintered at 1275 °C was 81.36 MPa and 1.975 g/cm^3, respectively. Mao *et al*. [31] employed the spontaneous coagulation casting (SCC) method, using APTMS as a surface modification. After sintering at 1260 °C for 4 h, the fused silica ceramics (50 vol.% solid content) showed a high bending strength of 61.59 MPa. Clegg *et al*. [32] used an improved process (with the help of a polymer solution additive) for making dense vitreous silica from submicrometer particles by sintering near 1000 °C and the measured strength value was 150 MPa.

Figure 5a shows the overview of the microstructure of the FS1100 sample, which contains grain sizes between 2–20 µm with intergranular pores. The amount of PDMS-derived silica particles is not large enough to fill the pores and merely form submicron islands on the surface of fused silica (Fig. 5a). Figure 5b shows SEM micrograph of the FS1200 sample in which PDMS-derived silica creates a liquid phase and covers the surface of fused silica particles. The presence of liquid phase at the surface of fused silica particles is more obvious in SEM image of the FS80201200 sample (Fig. 5c). It was shown that higher amounts of PDMS-derived silica melted, covering the surface of the fused silica grains, connecting the grains, and filling the pores to some extent. This can be the reason for the not much lower density and MOR strength of the FS80201200 sample despite its higher PDMS content compared with the FS1200 sample. In fact, this helps the grains form thicker necks, as shown in the FESEM image and yields higher strength.

IV. Conclusions

Mixing polydimethylsiloxane (PDMS) with the commercial fused silica helps in the formation of silica bodies with different shapes, which is very useful

especially when hollow slip-casting technique is not applicable. The PDMS curing provides the initial green strength necessary for fabricating specimens with uniform shapes. After sintering, submicron PDMS-derived silica particles are formed, but cannot efficiently fill the pores between coarse fused silica particles. XRD results revealed that the PDMS-derived silica crystallizes at 1100 °C and the amount of cristobalite phase increase with sintering temperature. The bulk density of the samples is in the range of 1.48–1.66 g/cm^3 with maximal value at 1300 °C, but this sample still has a high portion of porosity (about 24 vol.%). At sintering temperatures ≥1200 °C, submicron PDMS-derived silica particles melted and could bind the fused silica grains together which contribute to increase the strength (MOR). The MOR and density dropped with the increase of PDMS content to 20 wt.%. However, this decrease is not pronounced since higher amount of porosity in this sample is compensating with enhanced liquid phase sintering. Compared with other processing methods, this method provides less density and strength with more tendency to crystallize. This approach is promising, especially for preparing porous fused silica materials used as high-temperature filters and membranes.

Acknowledgments: The authors would like to acknowledge Pooyandegan Sanat Aria Corporation for supporting this research.

References

1. J.C. Sänger, B.R. Pauw, B. Riechers, A. Zocca, J. Rosalie, R. Maaß, H. Sturm, J. Günster, "Entering a new dimension in powder processing for advanced ceramics shaping", *Adv. Mater.*, **35** [8] (2023) 108–116.
2. M. Gromada, A. Tłuczek, R. Cygan, "Silica-based ceramic cores for high-pressure turbine airfoil blades in aircraft engines", *Process. Appl. Ceram.*, **18** [3] (2024) 299–306.
3. Y. Dai, Y. Yin, X. Xu, S. Jin, Y. Li, H. Harmuth, "Effect of the phase transformation on fracture behaviour of fused silica refractories*J.*. *Eur. Ceram. Soc.*, **38**, [16] (2018) 5601–5609.
4. L.A. Moore, C.M. Smith, "Fused silica as an optical material", *Opt. Mater. Express*, **12** [8] (2022) 3043–3059.
5. Z. Hu, Z. Yu, T. Zhao, D. Ding, X. Lv, Y. Ji, L. Peng, D. Yang, X. Yu, "Study on the mechanism of second phase formation in high-purity fused silica materials for semiconductor application", *J. Non-Cryst. Solids*, **635** (2024) 122990.
6. X. Li, J. Xu, A. Zhang, H. Peng, J. Zhang, Y. Li, M. Hu, Z. Lin, Y. Song, W. Chu, Z. Wang, Y. Cheng, "Laser multifunctional fabrication of metallic microthermal components embedded in fused silica for microfluidic applications", *Opt. Laser Technol*., **144** (2021) 107413.
7. N. Abbas, M. Luqman, A. Rauf, M. Shuaib, H. Haroon, S. Khalid Shah, M. Saleem, "Effect of boron oxide addition on microstructure and mechanical properties of slip cast fused silica", *Mater. Sci. Forum*, **1067** (2022) 227–231.
8. Y. Hu, Q. Zhang, Y. Feng, C. Wan, X. Sun, J. Duan, "The effects of PEG molecular weight on fused silica glass sintering by using nano silicon oxide powder", *J. Sol-Gel Sci. Technol.*, **105** [1] (2023) 63–72.
9. S. Yin, L. Guo, L. Pan, S. Yan, H. Qiao, S. Zhang, J. Tang, H. Min, T. Qiu, W. Wan, J. Yang, "Porous fused silica ceramics prepared by gelcasting using multigrade fused silica powders", *J. Alloys Compd.*, **819** (2020) 235–243.
10. P. Dehghani, F. Soleimani, "Effects of sintering temperature and cristobalite content on the bending strength of spark plasma sintered fused silica ceramics", *Ceram. Int.*, **48** [12] (2022) 16800–16807.
11. D.C. Jia, Y. Zhou, T.C. Lei, "Ambient and elevated temperature mechanical properties of hot-pressed fused silica matrix composite", *J. Eur. Ceram. Soc.*, **23** [5] (2003) 801–808.
12. D. Jia, L. Zhou, Z. Yang, X. Duan, Y. Zhou, "Effect of preforming process and starting fused SiO_2 particle size on microstructure and mechanical properties of pressurelessly sintered BNp/SiO_2 ceramic composites", *J. Am. Ceram. Soc.*, **94** [10] (2011) 3552–3560.
13. A.G. Eremeev, S.V. Egorov, A.A. Sorokin, Yu.V. Bykov, K.I. Rybakov, "Apparent viscosity reduction during microwave sintering of amorphous silica", *Ceram. Int.*, **44** [2] (2018) 1797–1801.
14. R.C. Breneman, J.W. Halloran, "Effect of cristobalite on the strength of sintered fused silica above and below the cristobalite transformation", *J. Am. Ceram. Soc.*, **98** [5] (2015) 1611–1617.
15. P. Dehghani, F. Soleimani, "Effect of cristobalite content on physical, dielectric constant, and bending strength of fused silica ceramics formed by slip casting method", *Adv. Ceram. Prog.*, **7** [2] (2021) 16–22.
16. W. Wan, C. Huang, J. Yang, J. Zeng, T. Qiu, "Effect of sintering temperature on the properties of fused silica ceramics prepared by gelcasting", *J. Electron. Mater.*, **43** [7] (2014) 2566–2572.
17. A. Kazemi, M.A. Faghihi-Sani, H.R. Alizadeh, "Investigation on cristobalite crystallization in silica-based ceramic cores for investment casting", *J. Eur. Ceram. Soc.*, **33** [15-16] (2013) 3397–3402.
18. R. Manivannan, A. Kumar, Ch. Subrahmanyam, "Aqueous gelcasting of fused silica using colloidal silica binder", *J. Am. Ceram. Soc.*, **96** [8] (2013) 2432–2436.
19. P. Colombo, G. Mera, R. Riedel, G.D. Sorarù, "Polymer-derived ceramics: 40 years of research and innovation in advanced ceramics", pp. 245–320 in *Ceramics Science and Technology*, Vol **7**, Wiley-VCH Verlag GmbH & Co. KGaA, 2013.
20. H. Elsayed, P. Colombo, E. Bernardo, "Direct ink writing of wollastonite-diopside glass-ceramic scaffolds from a silicone resin and engineered fillers", *J. Eur. Ceram. Soc.*, **37** [13] (2017) 4187–4195.
21. H. Elsayed, P. Rebesan, M.C. Crovace, E.D. Zanotto, P. Colombo, E. Bernardo, "Biosilicate® scaffolds produced by 3D-printing and direct foaming

using preceramic polymers", *J. Am. Ceram. Soc.*, **102** [3] (2019) 1010–1020.

22. A. Paryab, T. Godary, S. Abdollahi, M. Anousheh, A.M. Khachatourian, "Manufacturing and structural evaluation of polymer derived SiOC/TiC and SiOC/TiC/mullite nanocomposites", *Iran. J. Mater. Sci. Eng.*, **18** [3] (2021) 1–8.
23. A. Paryab, T. Godary, R. Khalilifard, A.M. Khachatourian, F. Abdollahi, S. Abdollahi, "The effect of Ag incorporation on the characteristics of the polymer derived bioactive silicate phosphate glass-ceramic scaffolds", *Bol. Soc. Esp. Cerámica Vidr.*, **61** [6] (2021) 653–662.
24. S. Abdollahi, A. Paryab, R. Khalilifard, M. Anousheh, A. Malek Khachatourian, "The fabrication and characterization of bioactive Akermanite/Octacalcium phosphate glass-ceramic scaffolds produced via PDC method", *Ceram. Int.*, **47** [5] (2021) 6653–6662.
25. A. Paryab, M. Saghatchi, S. Behsam, S. Abdollahi, A. Malek Khachatourian, "Large scale synthesis of mesoporous and nonporous silica submicron particles via polymer-derived ceramic method," *Int. J. Appl. Ceram. Technol.*, **21** [3] (2024) 1366–1371.
26. D. Kićević, M. Gašić, D. Marković, "A statistical analysis of the influence of processing conditions on the properties of fused silica", *J. Eur. Ceram. Soc.*, **16** [8] (1996) 857–864.
27. L.-Y. Wang M.-H. Hon, "The effect of cristobalite seed on the crystallization of fused silica based ceramic core - A kinetic study", *Ceram. Int.*, **21** [3] (1995) 187–193.
28. M. Romero, M. Kovacova, J. M. Rincón, "Effect of particle size on kinetics crystallization of an iron-rich glass", *J. Mater. Sci.*, **43** (2008) 4135–4142.
29. W. Duan, Z. Yang, D. Cai, J. Zhang, B. Niu, D. Jia, Y. Zhou, "Effect of sintering temperature on microstructure and mechanical properties of boron nitride whisker reinforced fused silica composites", *Ceram. Int.*, **46** [4] (2020) 5132–5140.
30. W. Wang, J. Yang, J. Zeng, T. Qiu, "Gelcasting of fused silica glass using a low-toxicity monomer DMAA", *J Non-Cryst. Solids*., **379** (2013) 229–234.
31. D. Mao, S. Yin, X. Fang, Y. Wang, Q. Li, J. Yang, "Preparation and properties of fused silica ceramics by Isobam spontaneous coagulation casting", *Ceram. Int.*, **48** [4] (2022) 5130–5138.